which simultaneously depopulates a Cr–Cr antibonding orbital and populates a Cr–Cr bonding orbital, will then strengthen the Cr–Cr interaction in opposition to a dimer disruption. From the low quantum yield for dimer disruption in $(\mu\text{-H})Cr_2(CO)_{10}^-$ and the Cr–Cr bonding feature of the Xα–SW LUMO $18a_1$, one must conclude that the Cr–Cr bonding interaction in the lowest excited state of this complex is significant.

The $16b_1 \rightarrow 18a_1$ transition is also consistent with the high quantum yield observed for the photosubstitution of CO. This transition depopulates $16b_1$ and thus weakens the σ-bonding between the Cr $3d_\pi$ and CO 2π orbitals; the effect is enhanced by populating $18a_1$, which is clearly $Cr–CO_t$ σ-antibonding. It is interesting to note that the $d_\pi \rightarrow 2\sigma$ transition deduced from the simple bonding scheme in Figure 3 also permits a facile CO dissociation as the d_π orbitals are depopulated.

So far as the photodissociation of CO is concerned, an apparent anomaly exists between the Xα–SW prediction of a trans-CO dissociation and the observed substitution of a cis CO. A plot of $18a_1$ in a xy plane containing four cis CO's and one Cr reveals that the CO's are σ-bonding to the Cr.[10] Therefore, a $16b_1 \rightarrow 18a_1$ transition should not directly effect a cis-CO dissociation. Experimentally, it is known that complexes like $(\mu\text{-H})Cr_2(CO)_{10}^-$ are very fluxional; thus it is conceivable that a trans CO is lost upon irradiation, and a subsequent rearrangement of the resultant $HCr_2(CO)_9^-$ species takes place.[21] The event could then lead to a final product that appears to have originated from a cis-Co photodissociation.

Acknowledgment. We are indebted to Professor S. Doniach, Professor H. Schlosser, and Dr. D. K. Misemer for their valuable assistance with the Xα–SW programs. We also thank Professor J. G. Norman, Jr., for a very helpful correspondence.

Registry No. $(\mu\text{-H})Cr_2(CO)_{10}^-$, 73740-63-3.

Supplementary Material Available: Tables S-I (low-lying valence energy levels and sphere charge distributions) and S-II (core energy levels) for $(\mu\text{-H})Cr_2(CO)_{10}^-$ (1 page). Ordering information is given on any current masthead page.

(21) Darensbourg, D. J.; Murphy, M. A. *J. Am. Chem. Soc.* **1978**, *100*, 463; *Inorg. Chem.* **1978**, *17*, 884.

Contribution from the Department of Chemistry, University of New Brunswick, Fredericton, New Brunswick E3B 6E2, Canada

Gas-Phase Bihalide and Pseudobihalide Ions. An Ion Cyclotron Resonance Determination of Hydrogen Bond Energies in XHY^- Species (X, Y = F, Cl, Br, CN)

J. W. LARSON[1] and T. B. McMAHON*

Received August 30, 1983

Hydrogen bond energies in the homonuclear bihalide ions FHF^- and $ClHCl^-$, the mixed-bihalide ion $ClHF^-$, and the pseudobihalide ions $FHCN^-$ and $ClHCN^-$ have been determined from ion cyclotron resonance halide-exchange equilibria measurements. A correlation between shift in frequency in hydrogen bond motion relative to the free halogen acid and hydrogen bond strength is proposed, which allows prediction of hydrogen bond energies for the additional species $FHBr^-$, FHI^-, $ClHBr^-$, and $ClHI^-$. Empirical correlations of trends in hydrogen bond energies also allow predictions to be made for $BrHBr^-$, $BrHCN^-$, and $CNHCN^-$. Ab initio calculations have been used to determine that the shape of the potential energy well for proton motion in the bihalide ions is a single minimum one.

Introduction

The hydrogen bihalide ions, XHY^-, represent the simplest examples of strongly hydrogen-bonded species. Their linear, triatomic structure has made them readily amenable to structural characterization by neutron diffraction,[2,3] X-ray crystallographic,[4] and vibrational spectroscopic methods.[5-10] Many studies have shown that the bifluoride ion, FHF^-, is a linear, centrosymmetric anion, both in crystalline salts with alkali metals[2,3] and tetraalkylammonium cations[4] and under argon matrix isolation conditions.[11] Considerably less structural information has been available for the other homonuclear bihalide ions until recent matrix isolation studies by Ault and Andrews[12] and photoionization studies by Milligan and Jacox[9] and by Pimentel and co-workers.[8] Evans and Lo[5] found the infrared spectra of the bihalide ion to be very dependent on the environment of the ion. They postulated that the HCl_2^- and HBr_2^- ions existed in two forms, an asymmetric anion and a centrosymmetric species with a single minimum potential, the latter form being favored in solution and in salts with large cations. Under matrix isolation conditions, however, the only observable HCl_2^- or HBr_2^- anion is the centrosymmetric species.[8,9,12-14]

Much less was known about mixed-bihalide ions until recent argon matrix isolation experiments.[11,12,14] The results of these experiments have been interpreted as indicating that the XHY^- anions can exist in two spectroscopically detectable forms analogous to those of the homonuclear bihalides. The higher infrared absorption frequency has been assigned to a species with a double minimum potential well for the hydrogen bond stretching motion, while a lower frequency has been assigned to a species with a single minimum potential similar to the centrosymmetric anion of the symmetric bihalide anions. The

(1) On sabbatical leave from Marshall University, Huntington, WV.
(2) Ibers, J. A. *J. Chem. Phys.* **1964**, *40*, 402.
(3) McGaw, B. L.; Ibers, J. A. *J. Chem. Phys.* **1963**, *39*, 2677.
(4) McDonald, T. R. R. *Acta Crystallogr.* **1960**, *13*, 113.
(5) (a) Evans, J. C.; Lo, G. Y. S. *J. Phys. Chem.* **1967**, *71*, 3942. (b) Evans, J. C.; Lo, G. Y. S. *Ibid.* **1969**, *73*, 448. (c) Evans, J. C.; Lo, G. Y. S. *Ibid.* **1966**, *70*, 11.
(6) Nibler, J. W.; Pimentel, G. C. *J. Chem. Phys.* **1967**, *47*, 710.
(7) Salthouse, J. A.; Waddington, T. C. *J. Chem. Soc. A* **1966**, 28.
(8) (a) Noble, P. N.; Pimentel, G. C. *J. Chem. Phys.* **1968**, *49*, 3165. (b) Noble, P. N. *Ibid.* **1972**, *56*, 2088.
(9) (a) Milligan, D. E.; Jacox, M. E. *J. Chem. Phys.* **1970**, *53*, 2034. (b) Milligan, D. E.; Jacox, M. E. *Ibid.* **1971**, *55*, 2550.
(10) Ault, B. S. *Acc. Chem. Res.* **1982**, *15*, 103 and references contained therein.
(11) Ault, B. S. *J. Phys. Chem.* **1979**, *83*, 837.
(12) Ault, B. S.; Andrews, L. *J. Chem. Phys.* **1975**, *63*, 2466.
(13) Hunt, R. L.; Ault, B. S. *Spectrochem. Acta, Part A* **1981**, *37A*, 63.
(14) Ellison, C. M.; Ault, B. S. *J. Phys. Chem.* **1979**, *83*, 832.

0020-1669/84/1323-2029$01.50/0

Table I. Halide-Exchange Equilibria and Associated Thermochemical Data

equilibrium	K_{eq}	ΔG°_{298} [a]	ΔS° [b]	ΔH° [a]
$FHF^- + PF_3 \rightleftharpoons PF_4^- + HF$	2.3	−0.5	−3.6	−1.6
$FHF^- + HCN \rightleftharpoons FHCN^- + HF$	4.6	−0.9	−0.3	−1.0
$PF_4^- + HCN \rightleftharpoons FHCN^- + PF_3$	1.4	−0.2	3.3	0.6
$ClHCl^- + HCO_2H \rightleftharpoons HCO_2HCl^- + HCl$	34.7	−2.1	−0.6	−2.3
$ClHCl^- + CH_3CO_2H \rightleftharpoons CH_3CO_2HCl^- + HCl$	3.3	−0.7	−0.5	−0.8
$ClSO_2^- + HCl \rightleftharpoons ClHCl^- + SO_2$	6.4	−1.1	−2.7	−1.9
$ClHCN^- + SO_2 \rightleftharpoons ClSO_2^- + HCN$	3.3	−0.7	2.9	0.2
$CH_2FCH_2OHCl^- + HCN \rightleftharpoons ClHCN^- + CH_2FCH_2OH$	4.6	−0.9	1.3	−0.5
$ClSO_2^- + HF \rightleftharpoons ClHF^- + SO_2$	2.1	−0.4	−1.7	−0.9

[a] All values in kcal mol^{-1} at 298 K. [b] All values in cal mol^{-1} K^{-1}.

forms of the anion produced are apparently dependent on the cation present and the end of the bihalide ion it is associated with. Finally, argon matrix isolation studies have shown for the first time a bihalide ion containing a pseudohalogen, $FHCN^-$.[15] This species has been shown to be linear and noncentrosymmetric.

Despite the extensive structural and spectroscopic characterization of bihalide ions, relatively little of a quantitative nature is known about the strengths of the hydrogen bonds involved. Prior to their study by gas-phase ion molecule reaction techniques, all experimental hydrogen bond energy determinations involved a variety of assumptions of questionable validity. On the basis of estimates of crystal lattice energies of tetraalkylammonium bihalide salts, McDaniel[16] has assigned hydrogen bond energies to HCl_2^-, HBr_2^-, and HI_2^- of 14.2, 12.8, and 12.4 kcal mol^{-1}, respectively. In view of the high-pressure mass spectrometric work of Kebarle on the binding energy of Cl^- to HCl in the gas phase of 23.7 kcal mol^{-1},[17] McDaniel's values would appear to be too low. A large number of experimental[18-22] and theoretical[23-27] attempts to obtain the hydrogen bond energy in FHF^- has resulted in a range of values from 30 to 58 kcal mol^{-1}. Very recently we have used the ion cyclotron resonance exchange equilibrium technique to determine F^- binding energies of a large number of Brønsted acids, including HF, and obtained a hydrogen bond energy for FHF^- of 38.6 kcal mol^{-1}.[28] Our studies to date have revealed this to be the strongest hydrogen bond observed in accord with the theoretical prediction. We have also recently developed methods for examination of Cl^- exchange equilibria and applied these methods to a variety of halogen acids and HCN. In the present publication we wish to report the hydrogen bond energies obtained of F^- and Cl^- adducts of various halogen acids and HCN and to suggest correlations that allow prediction of hydrogen bond strengths in bihalide species not yet examined.

Experimental Section

All experiments were conducted at ambient temperature with an ICR spectrometer of basic Varian V-5900 design, extensively modified to permit routine operation in both conventional-drift and trapped-ion modes.[29]

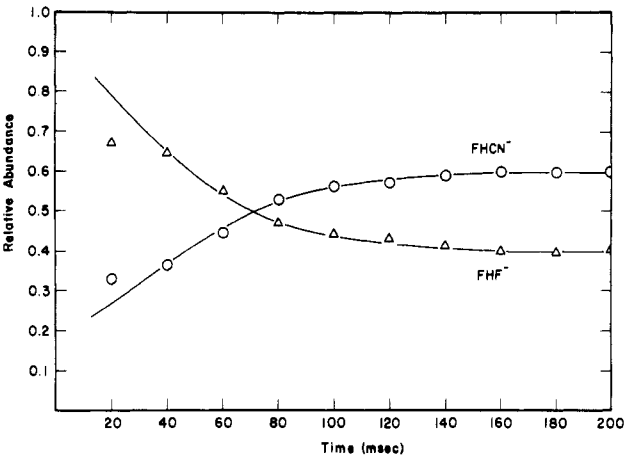

Figure 1. Variation of relative intensities of fluoride adducts of HF and HCN in a 1:6:28:7 mixture of NF_3:HCO_2CH_3:HF:HCN at a total pressure of 4.2×10^{-6} torr following a 5-ms, 70-eV electron beam pulse.

Except as stated otherwise, all materials were commercial samples of the highest purity obtainable and were used without further purification with the exception of degassing by successive freeze–pump–thaw cycles. HF, obtained from Matheson Canada Ltd., was transferred to a Monel vessel following removal of H_2 and SiF_4 impurities. HCN was synthesized by condensation of gaseous HCl into an aqueous solution of KCN and subsequent vacuum transfer of the volatile material.

Techniques for the bimolecular generation of F^- and Cl^- adducts have been described in detail previously.[28,30] Very briefly, F^- adducts were generated with use of the reaction of F^- with methyl formate (eq 1) followed by F^- transfer to the species of interest (eq 2).

$$F^- + HCO_2CH_3 \rightarrow F^-\cdots HOCH_3 + CO \quad (1)$$

$$F^-\cdots HOCH_3 + HX \rightarrow FHX^- + CH_3OH \quad (2)$$

Formation of Cl^- adducts was accomplished with use of the ion molecule reaction sequence observed in chloroformate esters[30] (eq 3 and 4), again followed by Cl^- transfer to species of interest (eq 5 and 6). Once F^- and Cl^- adducts of halogen acids and reference species had been obtained, halide ion exchange equilibria (eq 7) were used

$$Cl^- + ClCO_2F \rightarrow ClCO_2^- + RCl \quad (3)$$

$$ClCO_2^- + ClCO_2R \rightarrow Cl_2CO_2R^- + CO_2 \quad (4)$$

$$ClCO_2^- + HX \rightarrow ClHX^- + CO_2 \quad (5)$$

$$Cl_2CO_2R^- + HX \rightarrow ClHX^- + ClCO_2R \quad (6)$$

$$XHY^- + HZ \rightleftharpoons XHZ^- + HY \quad (7)$$

to obtain relative free energies of halide ion binding. Absolute binding energies of F^- and Cl^- to reference species have previously been determined by us.[28,30] A typical example of halide-exchange equilibria

(15) Ault, B. S. *J. Phys. Chem.* **1979**, *83*, 2634.
(16) McDaniel, P. H.; Vallee, R. E. *Inorg. Chem.* **1963**, *2*, 996.
(17) Yamdagni, R.; Kebarle, P. *Can. J. Chem.* **1974**, *52*, 2449.
(18) Waddington, T. C. *Trans. Faraday Soc.* **1958**, *54*, 25.
(19) Harrell, S. A.; McDaniel, D. H. *J. Am. Chem. Soc.* **1964**, *86*, 4497.
(20) Dixon, H. P.; Jenkins, H. D. B.; Waddington, T. C. *J. Chem. Phys.* **1972**, *57*, 4388.
(21) Jenkins, H. D. B.; Pratt, K. F. *J. Chem. Soc., Faraday Trans. 2* **1977**, *73*, 872.
(22) Harmon, K. M.; Lovelace, R. R. *J. Phys. Chem.* **1982**, *86*, 900.
(23) Noble, P. N.; Kortzeborn, R. N. *J. Chem. Phys.* **1970**, *52*, 5375.
(24) Almlof, J. *Chem. Phys. Lett.* **1972**, *17*, 49.
(25) Stogard, A.; Strich, A.; Roos, B.; Almlof, J. *J. Chem. Phys.* **1975**, *8*, 405.
(26) Emsley, J.; Hoyte, D. P. A.; Overill, R. E.; *J. Chem. Soc., Chem. Commun.* **1977**, 225.
(27) Emsley, J., private communication.
(28) Larson, J. W.; McMahon, T. B. *J. Am. Chem. Soc.* **1983**, *105*, 2944.
(29) McMahon, T. B.; Beauchamp, J. L. *Rev. Sci. Instrum.* **1973**, *43*, 509.
(30) Larson, J. W.; McMahon, T. B. *Can. J. Chem.* **1984**, *62*, 675.

Table II. Halide Ion Binding Energies for Hydrogen Halides, Hydrogen Cyanide, and Selected Reference Species

1. Bihalide Ions

XHY^-	$D(X^-\text{-HY})$, kcal mol^{-1}	$D(XH\text{-}Y^-)$, kcal mol^{-1}
FHF^- [a]	38.6	38.6
$FHCN^-$ [a]	39.5	21.1
$FHCl^-$ [a]	59.8	21.8
$FHBr^-$ [b]	65.0	17.0
FHI^- [b]	72.0	15.0
$ClHCl^-$ [a]	23.1	23.1
$NCHCl^-$ [a]	37.0	21.0
$ClHBr^-$ [b]	29.0	19.0
$ClHI^-$ [b]	32.0	13.0
$BrHBr^-$ [c]	20.0	20.0
$NCHBr^-$ [c]	42.0	16.0
$NCHCN^-$ [c]	20.0	20.0

2. Reference Species

M	$D(M\text{-}F^-)$,[d] kcal mol^{-1}	$D(M\text{-}Cl^-)$,[e] kcal mol^{-1}
PF_3	40.2	15.5
SO_2	43.8	20.9
CH_3CO_2H	44.1	23.9
HCO_2H	45.3	25.6
CH_2FCH_2OH	34.8	20.5

[a] Values obtained from halide binding energies as described in this work and from the difference in gas-phase acidities of HX and HY (Bartmess, J. E.; Scott, J. A.; McIver, R. T. *J. Am. Chem. Soc.* 1979, *101*, 6046). [b] Values obtained from correlations of $\Delta\nu$ vs. hydrogen bond strength as described in the text and from differences in gas-phase acidities of HX and HY. [c] Author's estimates based on empirical correlations as described in the text. [d] Reference 28. [e] Reference 30.

involving halogen acids is shown in Figure 1 for F^- transfer in HF–HCN mixtures.

Results

Halide ion transfer equilibria used to determine the hydrogen bond energies in the bihalide and pseudobihalide ions are summarized in Table I. Also included are the equilibrium constants obtained and the free energy changes derived. Entropy changes have been calculated by statistical thermodynamic methods as outlined elsewhere.[31] These values and the resulting enthalpy changes for halide exchange are summarized in Table I also. These data may then be used with the known halide ion binding enthalpy of the appropriate reference compound to obtain the halide ion binding energy of the halogen or pseudohalogen acid as well as the hydrogen bond energy in the bihalide ion. These values for bihalide ions and reference compounds are summarized in Table II. For these data it is important to distinguish between the individual halide ion binding energies and the strength of the hydrogen bond. For example, a given bihalide ion, XHY^-, may dissociate via two pathways (eq 8). If HX is a weaker gas-phase

$$XHY^- \rightarrow X^- + HY \quad (8a)$$

$$XHY^- \rightarrow HX + Y^- \quad (8b)$$

acid than HY, then the first path, (8a), will be more endothermic than the second, (8b). The less endothermic path then gives the strength of the hydrogen bond. These values are the second column of energies in Table II.

Discussion

Hydrogen Bond Energies. With the exception of Kebarle's work on $ClHCl^-$ using high-pressure mass spectrometry,[17] the present work provides the first quantitative data for hydrogen bond strengths in bihalide ions. As anticipated by predictions of classical inorganic chemistry and modern ab initio methods, the bifluoride ion, FHF^-, is seen to have the strongest hydrogen bond of any of the bihalide ions. In addition, our further investigations have revealed that it is in fact the strongest hydrogen bond of any yet examined. Within a homologous series of acids it has been shown that increases in fluoride binding energy are directly proportional to increases in gas-phase acidity.[28] However, the halogen acids and HCN do not constitute a homologous series. In addition to a dependence of fluoride binding energies on gas-phase acidity, we have previously shown that there is also a dependence upon the electronegativity of the atom or group to which the acidic proton is bound. The gas-phase acidities of the halogen acids investigated increase in the order HF < HCN < HCl < HBr < HI, while the electronegativities decrease in the order F > Cl > CN > Br > I. Thus the effect of increasing gas-phase acidity to increase halide ion binding energy is at least partially offset by decreasing electronegativity, which weakens the hydrogen bond to halide ions.

In a recent review, Ault[10] has noted that the change in frequency of the bihalide ion hydrogen bond stretching motion, relative to that in a free halogen acid, appears to correlate with the difference in proton affinities of the two halide ions involved. This proposal may be considered to be based on a combination of the increase in halide ion binding energy as the gas-phase acidity of the substrate halogen acid increases and the idea, attributable to Badger and Bauer,[32] that the strength of the hydrogen bond, $\Delta H°$, correlates with the shift of the hydrogen stretching motion, $\Delta\nu$. With accurate vibrational spectra of matrix-isolated bihalide ions now available[11-15] and the present determination of hydrogen bond strengths, we are in a position to rigorously test whether the $\Delta\nu$–ΔH correlations hold for these anions. These data have the advantage over previous tests of these correlations in that no solvent is involved to complicate matters. As shown in Figure 2, the $\Delta\nu$–ΔH correlation appears to be excellent for F^- and Cl^- adducts of HF since a straight line connecting the FHF^- and $FHCl^-$ points also intersect the origin, as it should.

Accepting the validity of the $\Delta\nu$ correlation with hydrogen bond strength, it is then possible to interpolate values of hydrogen bond energy for bihalide species not yet readily amenable to study by us. For example, the bihalide ions $FHBr^-$ and FHI^- are observable in the ICR spectrometer but no quantitative scale of Br^- and I^- binding energies has yet been developed. However, from the known vibrational spectra of these species, it is possible to predict that the hydrogen bond energies in $FHBr^-$ and FHI^- will be 17 and 15 kcal mol^{-1}, respectively. These predicted values are also summarized in Table II and are consistent with strengths anticipated for these hydrogen bonds. A similar argument may be pursued for halide ion adducts of HCl, although less quantitative data on hydrogen bond strengths is available. If a straight line is taken through the origin and the point for $ClHCl^-$, a tentative $\Delta\nu$ vs. hydrogen bond strength correlation may also be drawn. From the vibrational spectra of $ClHBr^-$ and $ClHI^-$, hydrogen bond strengths of 19 and 13 kcal mol^{-1} may then be interpolated. Given the errors inherent in a two-point straight line, the uncertainty in these values is somewhat greater.

Analysis of trends in hydrogen bond energies allows further predictions for other bihalide ions. For example, F^- is observed to be bound to HCN by 0.9 kcal mol^{-1} more than to HF while Cl^- is bound to HCN by 0.8 kcal less than to HF. Thus, it appears that anion binding energies to HF and HCN are

(31) Larson, J. W.; McMahon, T. B., submitted for publication in *J. Phys. Chem.*

(32) Badger, R. M.; Bauer, S. H. *J. Chem. Phys.* **1937**, *5*, 839.

(33) Shimanouchi, T. *Natl. Stand. Ref. Data Ser.* (*U.S., Natl. Bur. Stand.*) **1972**, *NSRDS-NBS 39*.

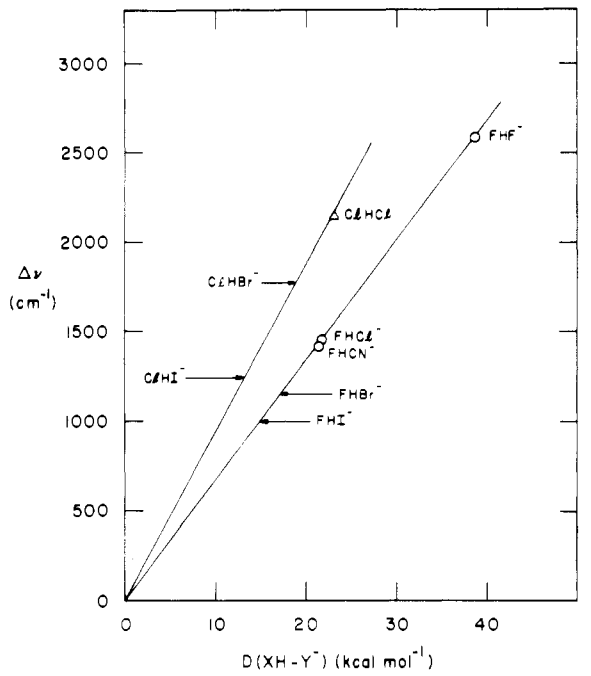

Figure 2. Correlation of shift in hydrogen bond stretching motion relative to the free halogen acid, $\Delta\nu$, with hydrogen bond strength for halide and cyanide adducts of HF and HCl. Arrows indicate hydrogen bond strengths interpolated from $\Delta\nu$ values reported in ref 10.

within ±1 kcal mol^{-1} of each other. With this trend, coupled with our failure to observe eq 9, it may be concluded that the

$$FHCN^- + HCN \not\rightarrow H(CN)_2^- + HF \qquad (9)$$

binding energy of CN^- to HCN is probably about 1 ± 1 kcal mol^{-1} less than that to HF and we hence assign a value of 20 kcal mol^{-1} to the hydrogen bond energy in $H(CN)_2^-$. Similarly, a value for hydrogen bond energy in $BrHCN^-$ of 16 ± 2 kcal mol^{-1} may be predicted from the $BrHF^-$ value on 17 ± 1 kcal mol^{-1}.

Finally, a value for hydrogen bond energy in $BrHBr^-$ of 20 ± 2 kcal mol^{-1} is predicted on the basis of the assumption that the binding energy of Br^- to HBr will be slightly greater than that to HCl 19 ± 2 kcal mol^{-1}).

Although the above predictions of hydrogen bond strengths are somewhat empirical, they do allow a prediction of the ability to synthesize as yet unobserved species. For example, the hydrogen bond energy in $ClHCN^-$ is comparable to that of $ClHF^-$ and hence $ClHCN^-$ should also be observable with use of the argon matrix isolation salt–molecule technique. Similarly, synthesis of the $BrHCN^-$ ion with a hydrogen bond strength between those of the already observed $FHBr^-$ and FHI^- species should also be feasible. In addition the bicyanide ion, $H(CN)_2^-$, predicted to be comparable in stability to HBr_2^-, would be a novel addition to the family of bihalide ions.

Potential Energy Surfaces. In argon matrix isolation experiments in which alkali-metal halides, MX, are covaporized with halogen acids, HY, to produce unsymmetrical bihalide ions, XHY^-, the vibrational data obtained suggest the presence of two different species.[12-14] The results obtained are essentially identical when synthesis of XHY^- via MY + HX is carried out. However, as the alkali metal, M, is varied, the relative amount of the two species produced appears to change. These data have been interpreted to indicate that the two species are the $M^+\cdots XHY^-$ and $M^+\cdots YHX^-$ ion pairs. This and additional deuterium-labeling studies suggest that the unsymmetrical bihalide ions have a double minimum potential well for hydrogen motion, thus allowing the two anions, $XH\cdots Y^-$ and $X^-\cdots HY$, to be trapped. In order to investigate

Table III. Variation of Total Energy for the $FHCl^-$ System as a Function of Hydrogen Position

r(F-H), Å	r(H-Cl), Å	energy, au[a]
0.85	2.11	−558.949 28
0.90	2.06	−558.958 52
0.9608	2.00	−558.961 76
1.00	1.95	−558.960 75
1.10	1.84	−558.952 05
1.20	1.72	−558.939 88
1.30	1.62	−558.927 85
1.40	1.54	−558.917 23
1.50	1.47	−558.908 07
1.60	1.43	−558.900 04
1.70	1.40	−558.892 87
1.80	1.37	−558.886 36
1.90	1.36	−558.880 38
2.00	1.34	−558.874 86

[a] 1 au = 627.5 kcal mol^{-1}.

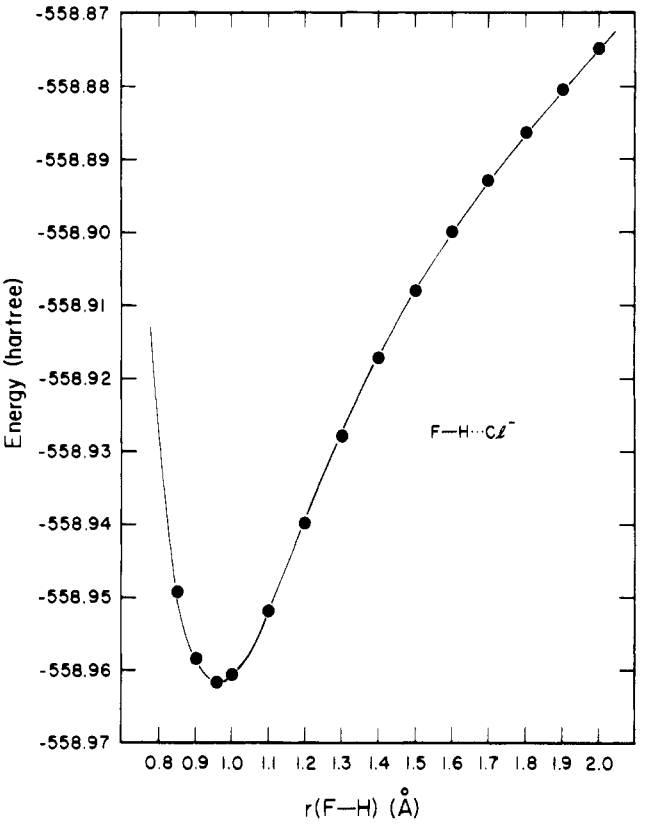

Figure 3. Potential energy profile for hydrogen motion in $FHCl^-$.

the nature of this potential energy surface further, we have carried out ab initio calculations of geometry and energetics of $FHCl^-$ and $FHCN^-$ using the GAUSSIAN 80[34] program package employing a 4-31G basis set.[35]

The potential surface for hydrogen motion in $FHCl^-$ was probed by choosing an F–H distance and then optimizing the H–Cl distance. The distances and energies obtained are summarized in Table III, and the potential energy profile is shown in Figure 3. It is evident that the isolated $FHCl^-$ exhibits a sharp single minimum potential well with an F–H distance very similar to that in neutral HF and a long H–Cl distance. This result is not unexpected for a system in which the proton is binding two anions of very different basicity.

Similar calculations were also carried out for $FHCN^-$ with the exception that in this case, because of computational ex-

(34) (a) Binkley, J. S.; Whiteside, R. A.; Krishnan, R.; Seeger, R.; de Frees, D. J.; Schlegel, H. B.; Topiol, S.; Kahn, L. R.; Pople, J. A. *QCPE* **1981**, *13*, 406. (b) van Kampen, P. N.; de Leeuw, F. A. A. M.; Smits, G. F.; Altona, C. *Ibid.* **1982**, *14*, 437.
(35) Ditchfield, R.; Hehre, W. J.; Pople, J. A. *J. Chem. Phys.* **1971**, *54*, 724.

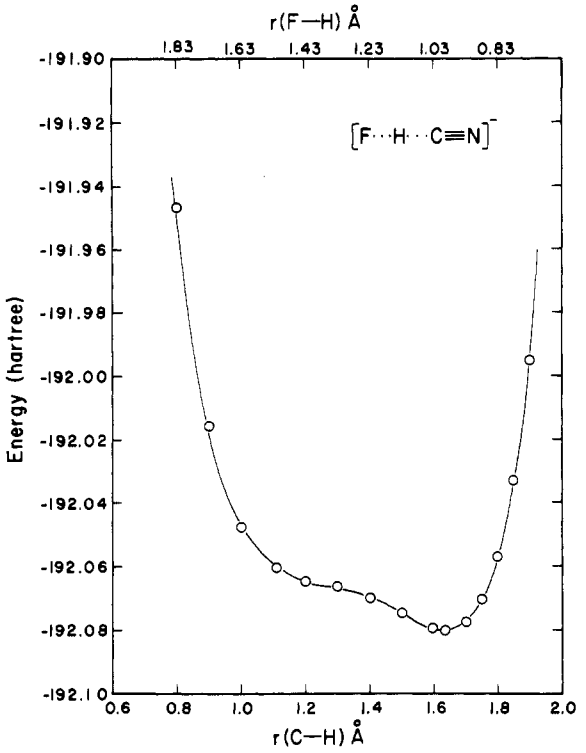

Figure 4. Potential energy profile for hydrogen motion in $FHCN^-$. Total F—C distance is fixed at 2.63 Å and C≡N distance at 1.16 Å.

pense, the total F—C and C≡N distances were held fixed at their optimized values of 2.63 and 1.16 Å, respectively, while the hydrogen position was varied. This appears to be a reasonable approximation since in the $FHCl^-$ case the total F–Cl distance remained reasonably constant over a wide range of hydrogen positions. The results for $FHCN^-$, shown in Figure 4, are very different than those for $FHCl^-$. Although a true double minimum potential well is not observed, a second "plateau" is seen corresponding roughly to F^-···HCN in addition to the true minimum corresponding roughly to FH···CN^-. This result is quite reasonable in view of the more similar basicities of F^- and CN^- relative to those of the FHCl case.

Although the ab initio results for these systems do not show double minimum potential wells, this does not preclude the possibility that such a situation does in fact exist in the species observed under argon matrix isolation conditions. In that medium a strongly polarizing alkali-metal cation is present which may dramatically alter the potential surface, giving rise to a double minimum potential well. The fact that two different types of anions are not reported for $FHCN^-$ may then simply be a result of a very low barrier between the minima produced.

Conclusion

Hydrogen bond strengths in five bihalide ions have been accurately established from ion cyclotron resonance halide-exchange equilibria. In addition, a proposed correlation between hydrogen bond strength and frequency shift of the hydrogen bond stretching motion relative to that in the free halogen acid has allowed prediction of a further four hydrogen bond strengths. With use of these data and empirical correlations, an additional three bihalide ion hydrogen bond strengths are proposed. These values allow us to suggest future directions for the synthesis of new bihalide ion species by using the argon matrix isolation salt–molecule technique. Lastly, ab initio calculations on the geometry and energetics of bihalide species have provided some insight into the nature of the potential energy surface for hydrogen bond motion.

Acknowledgment. The generous financial support of the Natural Sciences and Engineering Research Council of Canada (NSERC) is gratefully acknowledged. We thank U. Sishta, S. Morehouse, and Professor F. Grein for assistance with ab initio calculations and Professor W. V. F. Brooks for valuable discussions concerning vibrational spectra.

Registry No. HF, 7664-39-3; HCl, 7647-01-0; HBr, 10035-10-6; HI, 10034-85-2; HCN, 74-90-8; chloride, 16887-00-6; bromide, 24959-67-9; iodide, 20461-54-5; cyanide, 57-12-5; fluoride, 16984-48-8.

Contribution from the Institute for Physical Chemistry, University of Frankfurt, 6000 Frankfurt/Main, FRG, and Department of Chemistry and Quantum Institute, University of California, Santa Barbara, California 93106

Pressure Effects on the Photophysical and Photochemical Properties of the Rhodium(III) Ion $Rh(NH_3)_5Cl^{2+}$ in Nonaqueous Solvents

W. WEBER,[1] J. DiBENEDETTO,[2] H. OFFEN,[2] R. VAN ELDIK,*[1] and P. C. FORD*[2]

Received September 8, 1983

The effect of pressure was studied for the photosolvolysis reactions of $Rh(NH_3)_5Cl^{2+}$ in formamide, dimethylformamide, and dimethyl sulfoxide. The apparent volumes of activation for the chloride substitution quantum yields are −4.6 ± 0.7 and −7.8 ● 1.8 $cm^3\ mol^{-1}$ in FMA and Me_2SO, respectively. The corresponding values for the ammonia substitution quantum yields are +4.2 ± 0.9, +4.4 ± 0.9, and +6.3 ± 0.9 $cm^3\ mol^{-1}$ in FMA, Me_2SO, and DMF, respectively. The pressure dependence of the luminescence lifetimes was studied under comparable conditions, and the volumes of activation for τ^{-1} are −0.3 ± 0.4, −1 ● 1, and +1.3 ± 0.2 $cm^3\ mol^{-1}$ in FMA, Me_2SO, and DMF, respectively. These data enable the estimate of the volumes of activation for the individual ligand field excited-state deactivation processes, Cl^- labilization, NH_3 labilization, and nonradiative deactivation, from which the effect of the solvent can be deduced. Partial molar volume measurements and volume profile diagrams are used to discuss the intimate nature of the photosolvolysis processes.

Introduction

A recent article from these laboratories[3] reported the effects of pressure on the photochemical and photophysical properties of the rhodium(III) complexes $Rh(NH_3)_5Cl^{2+}$ and $Rh(NH_3)_5Br^{2+}$ and the perdeuterio analogues in aqueous solution. Analysis of the pressure effects on the luminescence lifetimes and the photoreaction quantum yields allowed the estimation of the volumes of activation (ΔV^*) for the individual deactivation processes of the lowest energy ligand field excited states (LEES). The ΔV^*_i vales for the ligand labilization pathways from the LEES, when interpreted in terms of hypothetical

(1) University of Frankfurt.
(2) University of California, Santa Barbara.
(3) Weber, W.; van Eldik, R.; Kelm, H.; DiBenedetto, J.; Ducommun, Y.; Offen, H.; Ford, P. C. *Inorg. Chem.* **1983**, *22*, 623.

0020-1669/84/1323-2033$01.50/0